Low-Leakage Superconducting Tunnel Junctions with a Single-Crystal Al_2O_3 Barrier*

S Oh[1,2], K Cicak[1], R McDermott[3], K B Cooper[3], K D Osborn[1], R W Simmonds[1], M Steffen[3], J M Martinis[3] and D P Pappas[1]

[1]National Institute of Standards and Technology, Boulder Colorado 80305

[2]Department of Physics, University of Illinois, Urbana Illinois 61801

[3]University of California, Santa Barbara California 93106

Abstract

We have developed a two-step growth scheme for single-crystal Al_2O_3 tunnel barriers. The barriers are epitaxially grown on single-crystal rhenium (Re) base electrodes that are grown epitaxially on a sapphire substrate, while polycrystalline Al is used as the top electrode. We show that by first growing an amorphous aluminum (Al) oxide layer at room temperature and crystallizing it at a high temperature in oxygen environment, a morphologically intact single-crystal Al_2O_3 layer is obtained. Tunnel junctions fabricated from these trilayers show very low subgap leakage current. This single-crystal Al_2O_3 junction may open a new venue for coherent quantum devices.

1. Introduction

A solid-state quantum bit (qubit) that has long coherence time and is easy to fabricate would be a significant breakthrough in the quantum computing field. To this end, various groups have recently implemented Josephson junction superconducting devices into qubits [1-6]. Before a multi-qubit quantum computer is realized, however, many obstacles need to be overcome. The most significant problem with any solid-state qubit implementation is strong coupling to environmental decoherent sources. Accordingly, identifying and removing these sources is an important prerequisite for construction of a solid-state quantum computer. Among other things, all the present-day superconducting qubits use amorphous AlO_x as a tunnel barrier. However, there is growing evidence that the amorphous AlO_x tunnel barriers have undesirable two-level fluctuators that adversely affect the qubit [7-10]. Because the two-level fluctuators are believed to originate from a nonequilibrium structure of the amorphous material [11], it is speculated that single-crystal tunnel barriers such as sapphire (Al_2O_3) may reduce the density of two-level fluctuators and improve the qubit performance [7]. In this work, we report the first successful fabrication of low-leakage single-crystal Al_2O_3 tunnel junctions. This breakthrough will allow us to test whether the two-level fluctuators observed in superconducting qubits are originating from the amorphous AlO_x barriers or not.

Previous efforts to make single-crystal Al_2O_3 tunnel junctions were made in the mid 1980s [12]. In this prior work, a thin (< 5 nm) Al layer was deposited at room temperature (RT) on epitaxially grown superconducting base layers and thermally oxidized at RT [13]. Although the Al-oxide formed in this manner showed some evidence of epitaxial texture, the degree of crystallinity was minimal because of the absence of lattice matching between Al and Al-oxide and the low oxide formation temperature. Moreover, the Al was deposited at a slow rate (< 3 nm/min) in the earlier work, which was necessary for epitaxial Al. However, we have found that, under these circumstances, the Al tends to ball up, and does not uniformly cover the base layer. In fact, this effect is exacerbated when using evaporation rather than sputtering, probably because the high kinetic energy inherent with sputtering helps smooth the film [12]. Such incomplete coverage of the base layer cannot be corrected during the oxidation process and results in leaky junctions [12]. These effects most likely explain the failure to obtain high-quality junctions in earlier investigations.

In order to overcome the limitations of conventional thermal oxidation schemes, we employed a reactive-evaporation technique [14] for the Al-oxide growth; Al was slowly (< 0.2 nm/min) evaporated in low pressure of molecular oxygen (typically, 1×10^{-6}

Torr). In this low-pressure oxygen environment, Auger electron spectroscopy (AES) study shows that while oxidation of the base layer is negligible, the deposited Al atoms are fully oxidized. This practice solves most of the problems inherent with the thermal oxidation scheme for epitaxial Al-oxide growth for the following reasons. First, the Al-oxide can be directly lattice-matched to the base layer without a layer of metallic Al interfering between the two. Second, without the metallic Al layer (melting point, 660 °C), it is possible to go to high temperatures to improve the crystalline quality of the Al-oxide (melting point, 2054 °C). Third, because Al-oxide has much lower mobility than free Al atoms, evaporated Al-oxide can uniformly cover the base layer without the balling-up problem. One property of the reactive-evaporation scheme is that the oxide thickness is linearly proportional to the evaporation time, in contrast to the self-limited logarithmic dependence in the thermal oxidation. Therefore, reproducible and stable evaporation rate control is critical. In fact, with existing technology this is straightforward using, for example, a modern Knudsen-cell evaporator, with which atomic-layer thickness control is commonly achieved [14].

2. Growth overview of the tunnel junction trilayer

The trilayer is composed of an epitaxial Re base electrode, an epitaxial Al_2O_3 tunnel barrier and a polycrystalline Al counter-electrode; in short epi-Re/epi-Al_2O_3/poly-Al. Re has several favorable properties as the base electrode for a single-crystal Al_2O_3 tunnel junction. First, its high melting point (3186 °C) enables high temperature growth for the single-crystal barriers. Second, the lattice spacing of its hexagonal close packed (hcp) structure (a=2.76 Å) is well matched with the oxygen sublattice (a=2.77 Å) of Al_2O_3 (0001) [15]. In addition, Re has a high enough superconducting critical temperature (T_c = 1.4~2.5 K) [16, 17] to be compatible with the present qubit technology [7]. Finally, under the same oxidation conditions, Re has a weaker tendency to oxidize than other common elemental superconductors such as Nb [18], and thus oxidation of the base Re layer can be easily avoided.

All three layers were grown *in situ* in an ultra high vacuum (UHV) system with a nominal base pressure of ~1×10^{-10} Torr. First, a 120~150 nm thick epitaxial Re layer was grown with DC magnetron sputtering on the 15 mm × 15 mm C-plane (0001) sapphire (Al_2O_3) substrate. On this substrate, epitaxial Re (0001) is obtained at 850 °C and a deposition rate of 0.3 Å/s [19]. Immediately after the base Re growth, it was annealed at 1050 °C for 20 minutes to increase its thermal stability during the following barrier layer

step. The next layer, Al_2O_3 barrier, is the main subject of this work and is described below in detail. Briefly, amorphous AlO_x was grown at a rate of 0.1~0.2 nm/min using the reactive-evaporation scheme. This was followed by a high-temperature annealing in order to crystallize the amorphous AlO_x into a single-crystal Al_2O_3. After the sample was cooled to room temperature (or near liquid nitrogen temperature for smoother morphology of the top Al layer) and the background pressure dropped below 5×10^{-9} Torr, the top Al layer was thermally evaporated at a faster rate (~3 nm/min) to about 100 nm thick. Under these conditions, the deposited Al is polycrystalline. At each step, the crystallinity of the film was checked by reflective high energy electron diffraction (RHEED) as shown in Fig. 1 and discussed below.

3. Detailed Al-oxide growth study

While epitaxial base Re growth is rather straightforward (see Fig. 1(a) and Fig. 2(a)), the growth of epitaxial Al_2O_3 barriers needs more care. Epitaxy of a film strongly depends on the substrate temperature, T_S. At room temperature, the reactive-evaporated Al-oxide yields an amorphous structure, which appears as a diffuse pattern in RHEED (see Fig. 1(b)). This implies that the Al atoms combine with oxygen atoms almost instantaneously

on the Re surface and do not have enough mobility to crystallize. A single-crystal RHEED pattern appears only for T_S 700 °C (see Fig. 1(c)) and becomes more pronounced as T_S is raised up to 800 °C (see Fig. 1(d)).

However, the atomic force microscopy (AFM) images shown in Fig. 2 demonstrate that unless the high temperature treatment is carefully optimized, surface morphology can degrade during the process. For example, when ~2 nm of Al-oxide was directly grown at 800 °C in 4×10^{-6} Torr of O_2, even though it showed a single-crystal RHEED pattern similar to Fig. 1(d), the oxide film formed three-dimensional (3D) clumps as shown in Fig. 2(b). The clumps are due most likely to the enhanced mobility of the adatoms at high temperatures. A common technique used to solve this problem is to grow the film at a low temperature and anneal it at a high temperature [20]. Accordingly, when ~2 nm of Al-oxide was first deposited at RT in 1×10^{-6} Torr of O_2 as an amorphous AlO_x and later annealed at 800 °C for a few minutes in UHV, a single-crystal RHEED pattern appeared. However, Fig. 2(c) shows that this Al-oxide still has 3D clumps on the surface. This image indicates that since amorphous AlO_x is oxygen-deficient, without ambient oxygen during the annealing the amorphous AlO_x cannot stoichiometrically crystallize into Al_2O_3. Based on this interpretation, we annealed the RT-grown

amorphous AlO_x in 4×10^{-6} Torr of O_2 at 800 °C. Under these conditions, the film was free of any morphological defects even after it crystallized, as shown in Fig. 2(d)).

While real-space information such as AFM is essential to solve morphological problems, the amorphous-to-epitaxial transformation is seen most easily in k-space as shown in the RHEED patterns of Fig. 1. When ~2 nm of AlO_x is deposited on the epitaxial Re layer at RT, the streaky diffraction pattern (Fig. 1(a)) from the Re layer is gone, and only a diffuse amorphous pattern (Fig. 1(b)) from AlO_x is observed. Annealing the amorphous oxide at 700 °C in O_2 brings a faint streaky pattern (Fig. 1(c)) out of the diffuse background, and when the annealing temperature is increased up to 800 °C in O_2, a clear single-crystal pattern (Fig. 1(d)) emerges. This sequence shows how the low-temperature growth followed by the high-temperature annealing transforms the amorphous AlO_x into the single-crystal Al_2O_3.

4. Junction fabrication and *I-V* measurement

After the top Al layer was deposited *in situ* near liquid nitrogen temperature, the trilayer was processed into tunnel junctions using a standard photolithography as briefly described below. First, junction structures were defined by Ar^+ ion-milling, and the base

wiring layer by SF_6 reactive-ion-etching (RIE). Then SiO_2 was deposited over the entire sample as an insulating layer, and via-holes were defined by $CHF_3 + O_2$ RIE for electrical contacts. Finally an Al wiring layer was defined by sputter deposition and wet-chemical etching. A finished junction pattern is shown in Fig. 3(a), and room temperature conductance measurements are shown as a function of junction area in Fig. 3(b). Overall, the conductance scales linearly with the junction area except for some scattering. The scattering may be due either to the stepped base Re morphology [19] or to evaporation source nonuniformity, and its exact origin is under investigation.

Fig. 4(a) and 4(b) show current-voltage (I-V) curves of a typical single-crystal Al_2O_3 tunnel junction taken at ~80 mK. One way to quantify the junction quality is to define a quality factor [12], $Q \equiv I_N/I_S$, where I_N is the normal current just above the gap voltage and I_S the subgap leakage current at half the voltage. This junction shows a $Q \equiv I_N$ (0.70 mV)/I_S(0.35 mV) of 1200. Although such a high quality factor is not uncommon among amorphous AlO_x junctions [22], it is unprecedented for a single-crystal Al_2O_3 junction. This high quality factor verifies that the density of pinholes is very small, as expected from the AFM study. The next step is to implement a qubit with this new

trilayer and study the role of single-crystal tunnel barriers with respect to the qubit performance.

5. Conclusion

Using a reactive-evaporation scheme, we have overcome the limitation of the conventional thermal oxidation technique and successfully grown superconducting tunnel junctions with a lattice-matched single-crystal Al_2O_3 barrier on an epitaxial Re base layer. We have shown that high temperature processes, which are necessary for single-crystal Al_2O_3 growth, tend to cause a 3D clumping problem. However, by annealing AlO_x in an O_2 background, clump-free single-crystal layers of Al_2O_3 have been obtained. Tunnel junctions made with these trilayers show a very high quality factor. Testing whether or not the single-crystal Al_2O_3 qubit shows fewer two-level fluctuators will be an important experimental step toward a coherent solid-state quantum computer.

Acknowledgements

We appreciate useful discussions with Paul Welander, J. N. Eckstein and Alexander Popov. We also thank Ben Mazin for measuring T_c of our Re films. This work was

supported by the National Security Agency (NSA) Advanced Research and Development Activity (ARDA) through Army Research Office grants W911NF-04-1-2004 and MOD717304, by the North Atlantic Treaty Organization (NATO) through Grant PST.CLG.979374, and by the National Institute of Standards and Technology (NIST).

References

[1] Chiorescu I, Nakamura Y, Harmans C J P M and Mooij J E 2003 *Science* **299** 1869

[2] Martinis J M, Nam S, Aumentado J and Urbina C 2002 *Phys. Rev. Lett.* **89** 117901

[3] Pashkin Yu A *et al* 2003 *Nature* **421** 823

[4] Yamamoto T, Pashkin Yu A, Astafiev O, Nakamura Y and Tsai J S 2003 *Nature* **425** 941

[5] Nakamura Y, Pashkin Yu A and Tsai J S 1999 *Nature* **398** 786

[6] Vion D *et al* 2002 *Science* **296** 886

[7] Simmonds R W, Lang K M, Hite D A, Nam S, Pappas D P and Martinis J M 2004 *Phys. Rev. Lett.* **93** 077003

[8] Shnirman A, Schön G, Martin I and Makhlin Y 2005 *Phys. Rev. Lett.* **94** 127002

[9] Bertet P *et al cond-mat*/0412485

[10] Plourde P L T *et al cond-mat*/0501679

[11] Phillips W A 1987 *Rep. Prog. Phys.* **50** 1657

[12] Braginski A I, Talvacchio J, Janocko M A and Gavaler J R 1986 *J. Appl. Phys.* **60** 2058

[13] Gurvitch M, Washington M A and Huggins H A 1983 *Appl. Phys. Lett.* **42** 472

[14] Oh S, Warusawithana M and Eckstein J N 2004 *Phys. Rev. B* **70** 64509

[15] Wu Y, Garfunkel E and Madey T E 1996 *J. Vac. Sci. Technol. A* **14** 2554

[16] Haq A U and Meyer O 1982 *Thin Solid Films* **94** 119

[17] T_c depends on the crystallinity of the sample; the measured T_c of our typical Re base layer was 1.95 K

[18] Samsonov G V 1982 *The Oxide Handbook*. (IFI/Plenum Data Company)

[19] Oh S *et al* submitted to *Thin Solid Films* in May 2005

[20] Smith A R, Chao K -J, Niu Q and Shih C -K 1996 *Science* **273** 223

[21] Klapwijk T M, Blonder G E and Tinkham M 1982 *Physica B* **109&110** 1657

[22] Lang K M, Nam S, Aumentado J, Urbina C and Martinis J M 2003 *IEEE Trans. Appl. Supercond.* **13** 989

Figure Captions

Figure 1: RHEED images of the epi-Re/epi-Al_2O_3 growth. (a) Epitaxial base Re. (b) ~2 nm of amorphous AlO_x grown at RT on the base epi-Re layer. No diffraction is seen except for a diffuse amorphous pattern. This also shows that 2 nm of AlO_x is thick enough to completely block any diffracted electrons from the base layer. (c) After a few minute annealing of AlO_x at 700 °C on epi-Re, a weak but discernible streaky pattern appears. This implies that AlO_x starts to crystallize at this temperature. (d) When the annealing temperature is increased to 800 °C, a complete single-crystal RHEED pattern appears. This sequence also verifies that the single-crystal RHEED pattern in (d) represents that of the Al_2O_3 barrier, and not that of the base Re through the thin barrier.

Figure 2: AFM images of the film morphology. (a) Re epitaxial base layer, which was grown at 850 °C on an Al_2O_3 (0001) substrate and annealed at 1050 °C for 30 minutes. (b), (c) and (d) are Al_2O_3 barriers grown ~2 nm thick on the base Re layer under different growth conditions, all of which showed single-crystal RHEED patterns similar to Fig. 1(d). (b) Grown at 800 °C in 4×10^{-6} Torr of O_2. Scattered 3D

clumps (pink in online images) are observed. (b) Grown at RT in 1×10^{-6} Torr of O_2 and annealed at 800 °C in UHV. 3D clumps still exist. (c) Grown at RT in 1×10^{-6} Torr of O_2 and annealed at 800 °C in 4×10^{-6} Torr of O_2. No morphological defects are observed.

Figure 3: (a) Processed junction geometry. (b) Conductance vs. Area. Except for some scattering, the conductance is roughly proportional to the junction area. The straight line is just a guide to the eye.

Figure 4: *I-V* curve taken at ~80 mK on an epi-Re/epi-Al_2O_3/poly-Al tunnel junction. (a) Linear vertical scale. (b) Logarithmic vertical scale: absolute value is used. This particular junction has an area of 160 μm^2 and a critical current of 14.9 μA. The sum-gap voltage, $\Delta_{Re} + \Delta_{Al}$, defined as the point of the highest slope is 0.68 mV. Based on the BCS gap formula, $\Delta=1.76k_BT_c$, and the T_c of the base Re, 1.95 K, the estimated T_c of the top Al layer is 2.5 K. The reason why this value is much larger than that of a typical Al film, which is 1.2 K, is that the top Al layer was deposited at near liquid nitrogen temperature and thus is disordered. The quality

factor defined as $Q \equiv I_N(0.70\ \text{mV})/I_S(0.35\ \text{mV})$ is 1200. The subgap structures seen in (b) are probably due to multiple Andreev reflections [21].

Figure 1

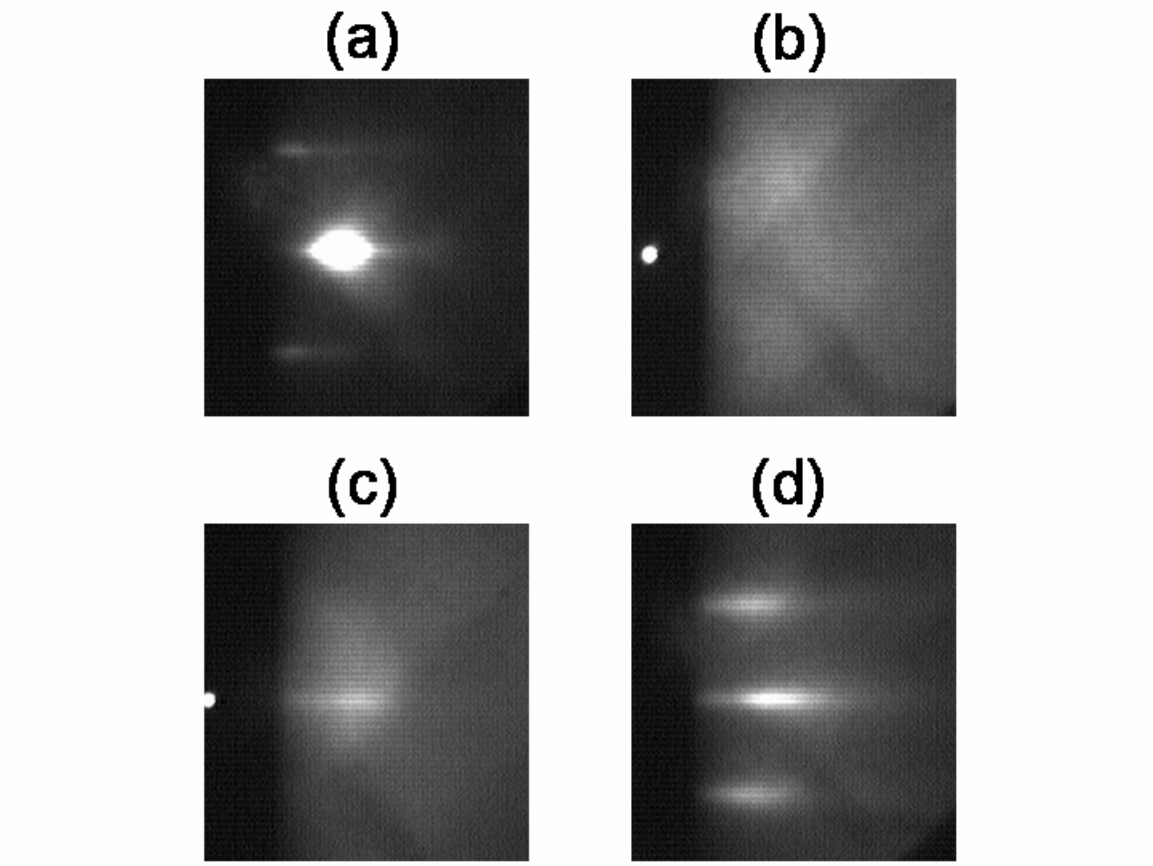

Figure 2

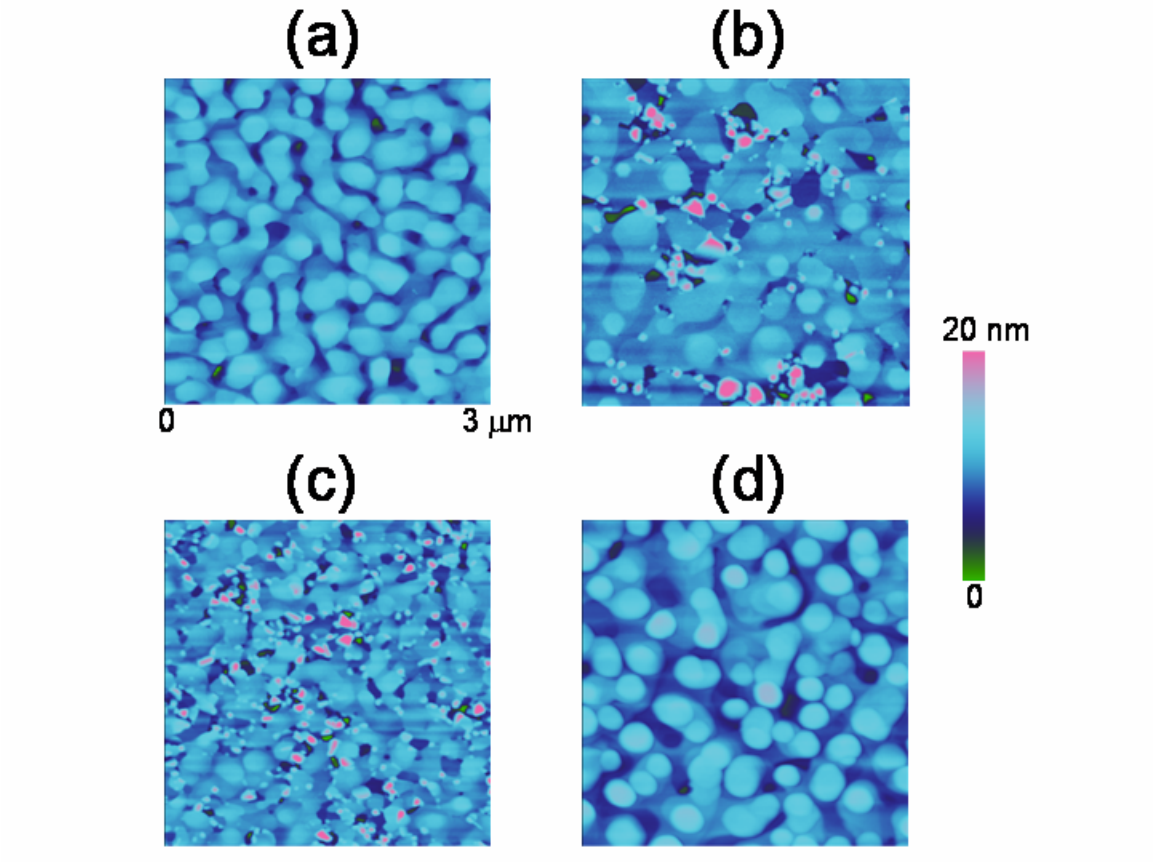

Figure 3

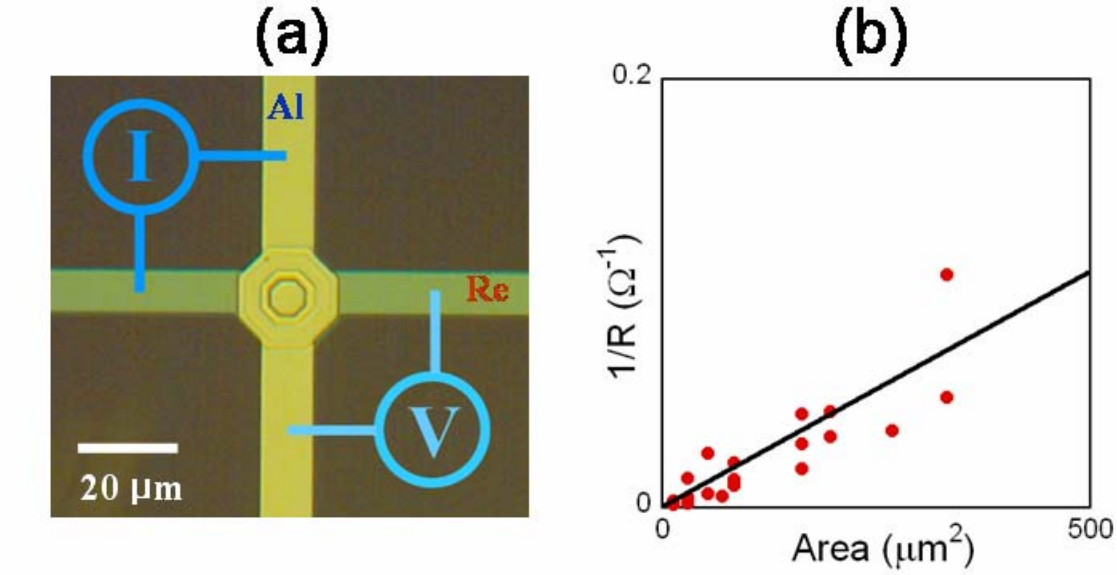

Figure 4

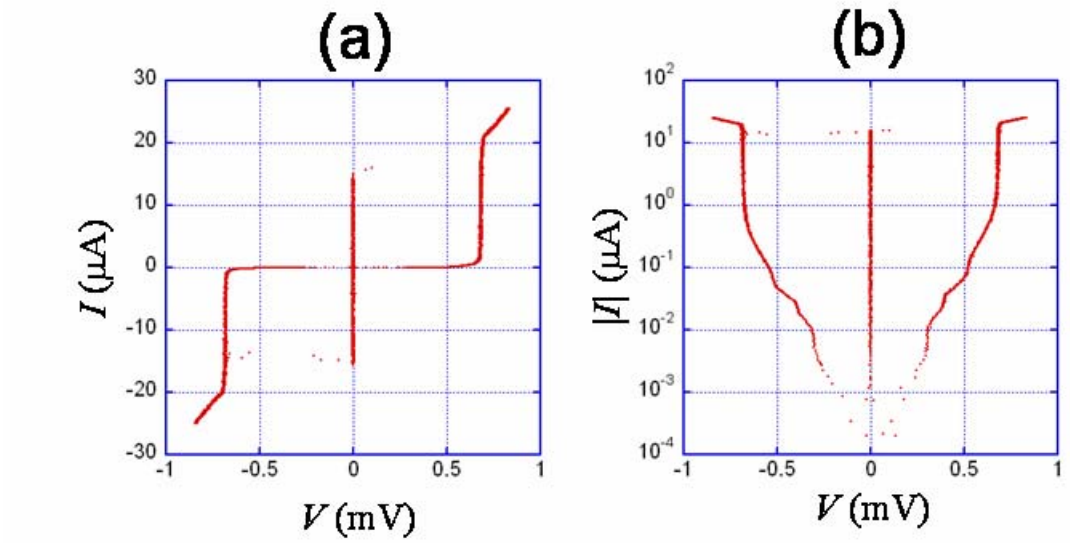
(a)
(b)
I (μA)
|I| (μA)
V (mV)
V (mV)
30
20
10
0
-10
-20
-30
-1
-0.5
0
0.5
1
10^2
10^1
10^0
10^-1
10^-2
10^-3
10^-4